Supporting Information

Efficient and Robust Manganese-Based Hybrid Ceramics Enabled by Dual-Ligand Regulation for High-Performance 3D X-ray Imaging

Jiankun Xue[a,c], Yaping Chen[a,c], Hao Lu[b]*, Chenrui Wang[a], Lian Wang[a,c], Guiqing Feng[a,c], Xin Huang[a], Yi Zheng[a], Min Chen[a], Xieming Xu[a,b]*, Shuaihua Wang[a,b] and Shaofan Wu[a]

[a]Key Laboratory of Optoelectronic Materials Chemistry and Physics, Fujian Institute of Research on the Structure of Matter, Chinese Academy of Sciences, Fuzhou, 350002, PR China

[b]Fujian Science & Technology Innovation Laboratory for Optoelectronic Information of China, Fuzhou, 350108, PR China

[c]University of Chinese Academy of Sciences, Beijing, 100049, PR China.

E-mail: xuxieming@fjoel.cn

Experimental Section

Materials: Methyl triphenyl bromophosphine (MTP, 99%) and benzyltrimethylammonium (BTAC) were purchased from Aladdin Company. Manganese bromide tetrahydrate ($MnBr_2 \cdot 4H_2O$) was supplied by Acros Company. All reagents and chemicals were used as received without further purification.

Synthesis of single crystals

Single crystals of $(MTP)_2MnBr_4$ and $(BTAC)_2MnBr_4$ were grown using the aqueous solution method. Under stirring conditions, $MnBr_2 \cdot 4H_2O$ (0.5 mmol), MTP (1 mmol) and BTAC (1 mmol) were separately dissolved in 99.9% anhydrous ethanol (2 mL). For the growth of MTP-BTAC$MnBr_4$, $MnBr_2 \cdot 4H_2O$ (0.5 mmol) and MTP (0.5 mmol), and BTAC (0.5 mmol) were dissolved together in 99.9% anhydrous ethanol (2 mL). After sealing pinholes with a thin film, the mixture was slowly evaporated at a constant temperature of 60°C in air for 4 days. Crystals of $(MTP)_2MnBr_4$, $(BTAC)_2MnBr_4$, and MTP-BTAC$MnBr_4$ crystals gradually precipitated and were collected.

Preparation of mixed metal halide ceramics

MHC were prepared by grinding organic ligands and manganese-based metal halides in a mortar under air conditions until uniform. The mixture was then transferred to a Petri dish and heated to 130°C. The melt was cooled to room temperature.

Fabrication of large-area MHC detectors

MTP-BTAC$MnBr_4$ scintillators are prepared by heating pre-fabricated ceramic precursors in an air atmosphere at temperatures between 130 and 150 °C for 30 minutes, until they reach a molten state. Optically graded quartz plates are then heated at 130 °C for 10 minutes. The molten ceramic precursor is then dispensed under controlled pressure onto an 8 cm × 8 cm quartz plate for one minute to ensure uniform distribution. Once cooled to room temperature, the assembly is encapsulated with UV adhesive to create a large-area MTP-BTAC$MnBr_4$ scintillation screen.

Material Characterization

PXRD patterns were collected using a Rigaku Miniflex 600. Absorption spectra were obtained by a UV-Vis-NIR spectrophotometer (Lambda 950). The thermogravimetric curves were obtained by a simultaneous thermal analyzer (STA 449F3) under the N2 atmosphere. Scanning electron microscope (SEM) images and EDS elemental maps were obtained using a Hitachi S4800 field emission scanning electron microscope.

X-ray Detection

We used a tungsten anode X-ray tube (Moxtek TUB00146-W06) to produce continuous 30-50 kV X-ray with a maximum output power of 12 W, and use of 2 mm and 10 mm thick aluminum plates to further control the radiation dose rate. A Keithley Model 2450 source meter was utilized to supply bias and detection response currents. During the test, the tube voltage of the X-ray source is kept constant and the tube current is varied to adjust the X-ray dose rate.

Figure S1. Schematic diagram of volatilization method

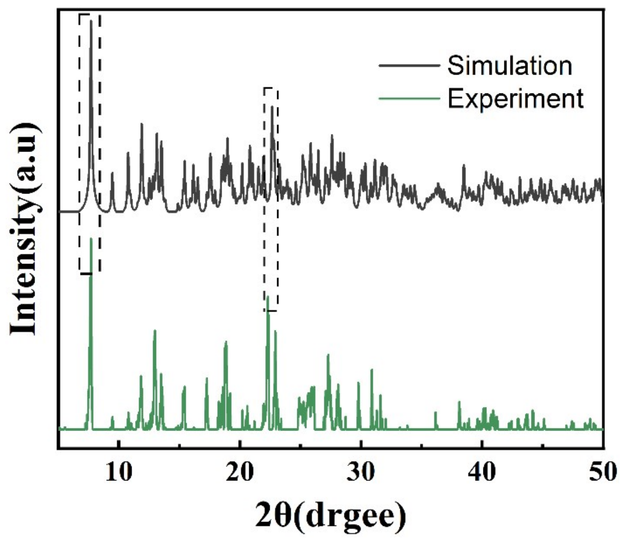

Figure S2. Characteristic analysis of XRD experiments and simulations for crystalline material MTP-BTACMnBr$_4$.

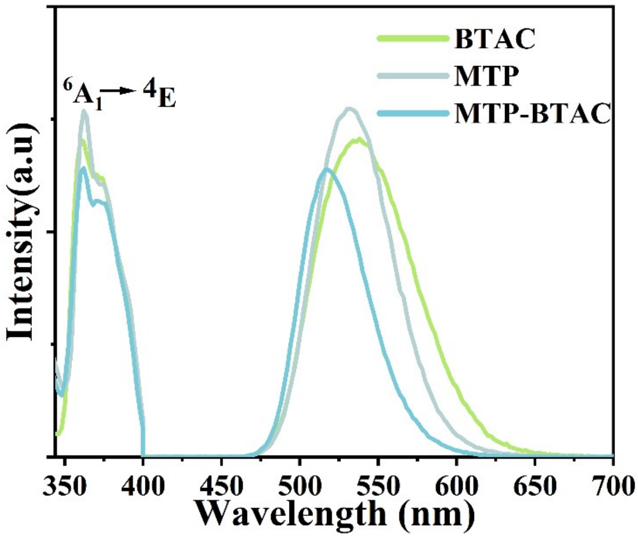

Figure S3. PL and PLE spectra of MTP-BTAC$MnBr_4$, $(MTP)_2MnBr_4$, and $(BTAC)_2MnBr_4$.

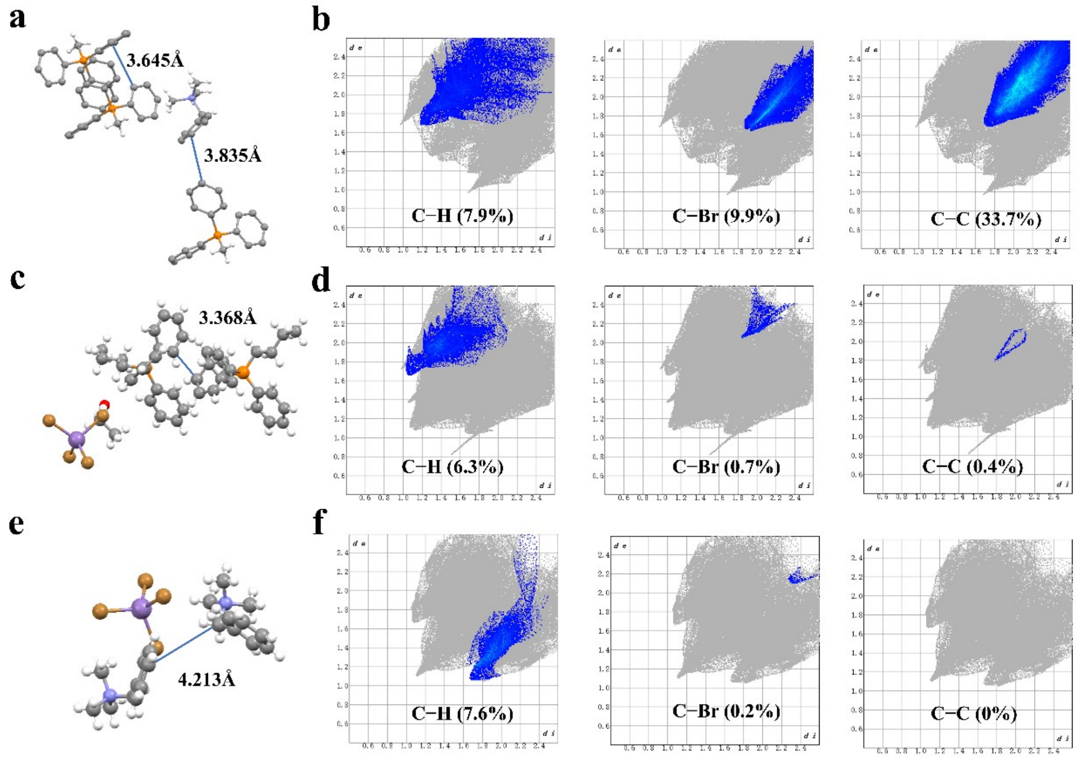

Figure S4. Hirschfeld surface-derived two-dimensional fingerprint plots.

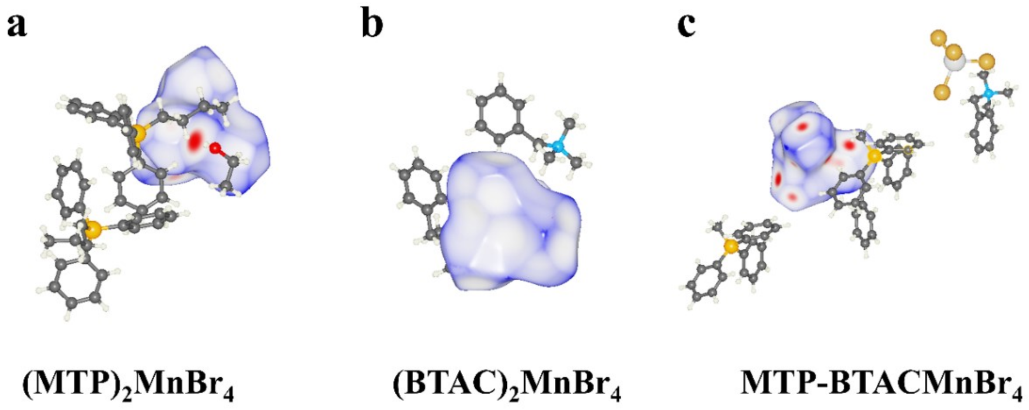

Figure S5. Distribution of forces surrounding $[MnBr_4]^{2-}$ in three materials

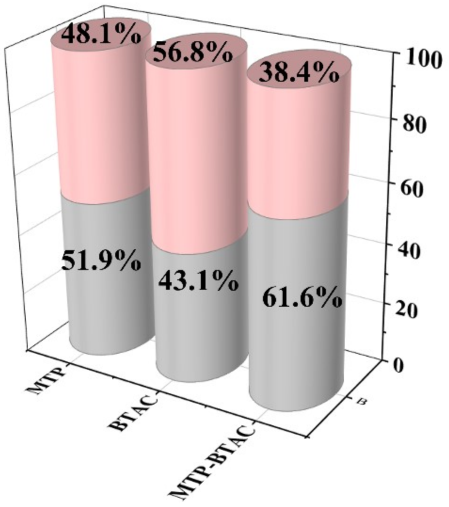

Figure S6. Free region and atom occupancy of these hybrid manganese bromides.

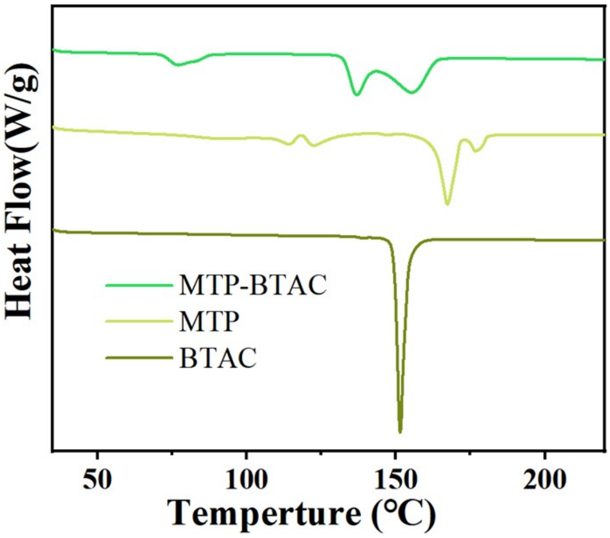

Figure S7. DSC curve of crystalline materials.

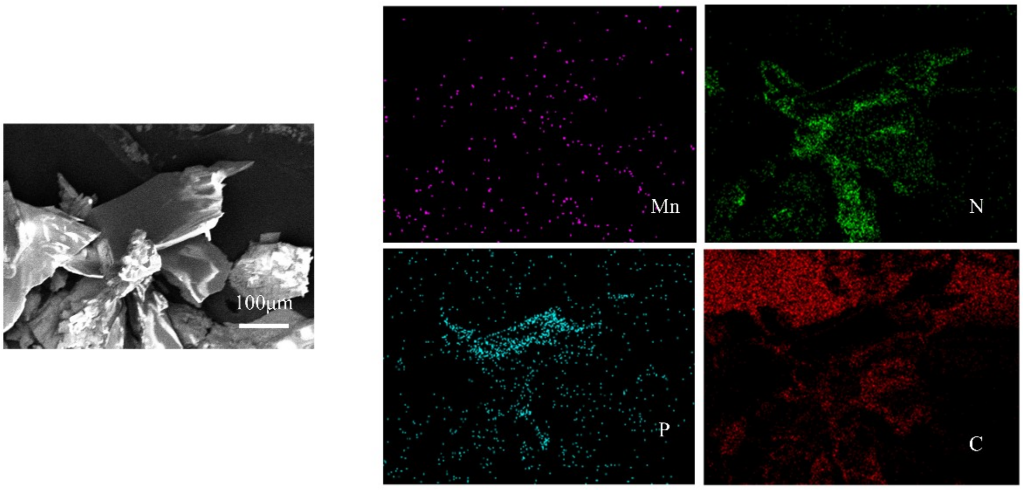

Figure S8. SEM images with elemental mappings of N, P, and Mn.

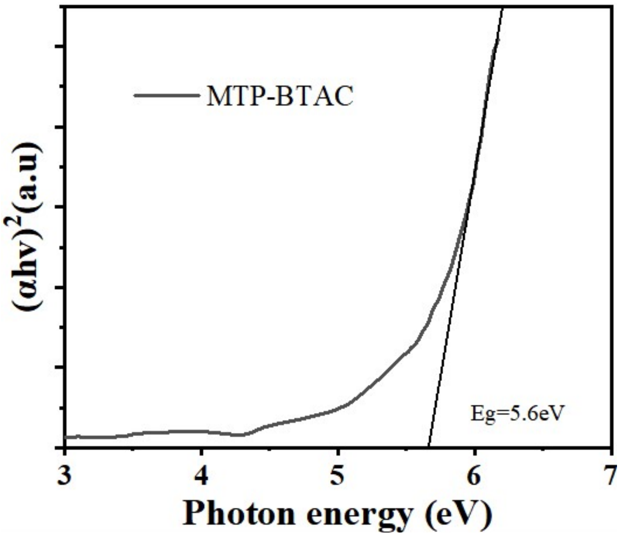

Figure S9. MTP-BTAC UV absorption spectrum.

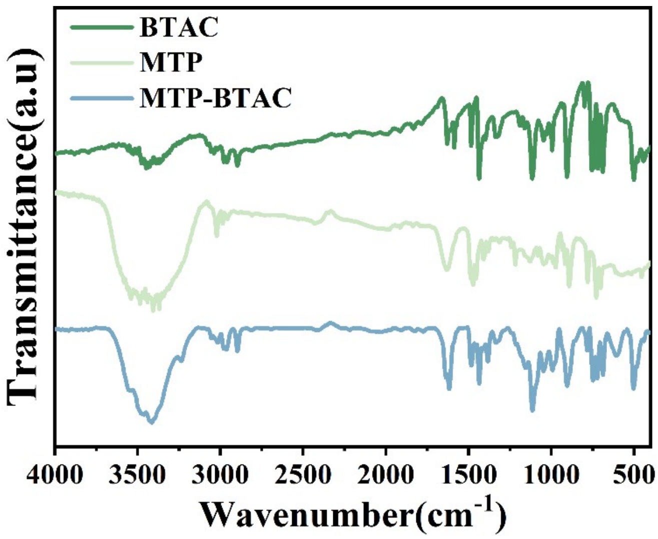

Figure S10. Infrared absorption spectra of MTP-BTACMnBr$_4$, (MTP)$_2$MnBr$_4$, and (BTAC)$_2$MnBr$_4$

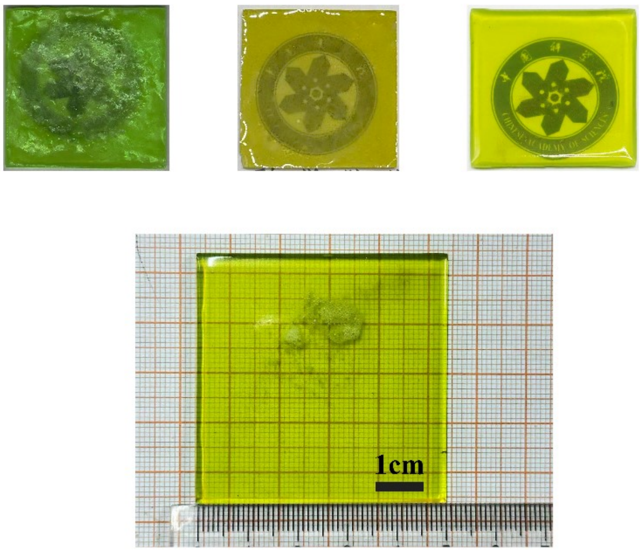

Figure S11. Physical Image of MHC Sample (From left to right: $(BTAC)_2MnBr_4$, $(MTP)_2MnBr_4$, MTP-BTACMnBr_4.

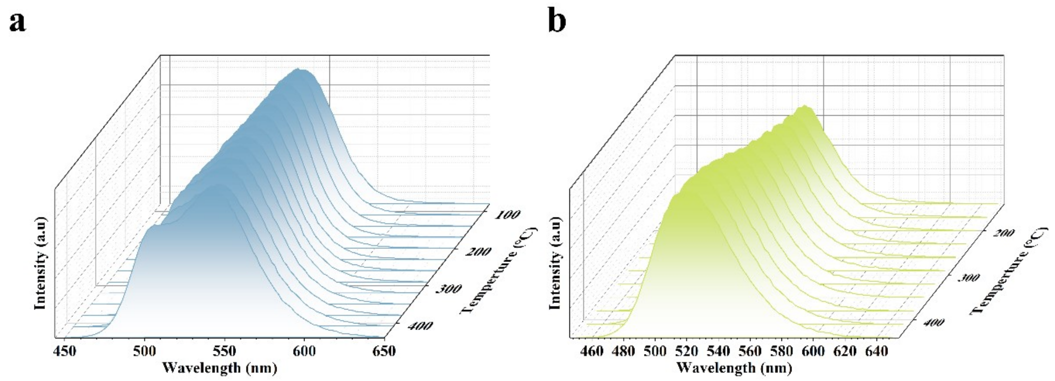

Figure S12. The variable temperature PL of $(MTP)_2MnBr_4$ and $(BTAC)_2MnBr_4$

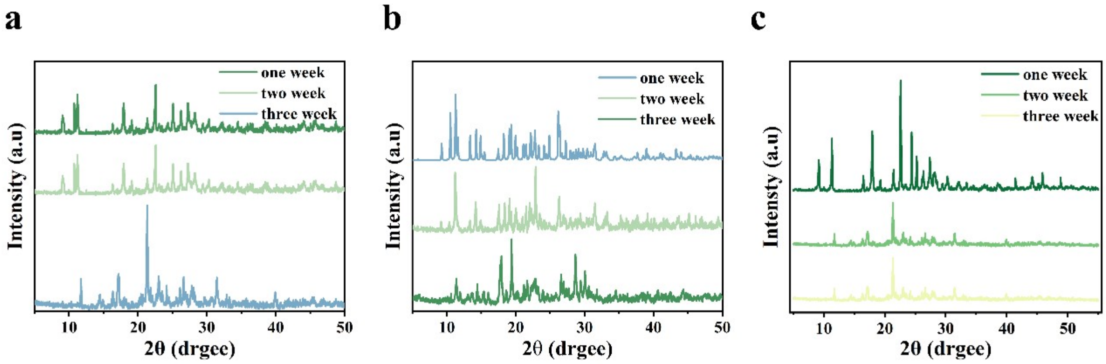

Figure S13. XRD patterns of materials at identical time intervals

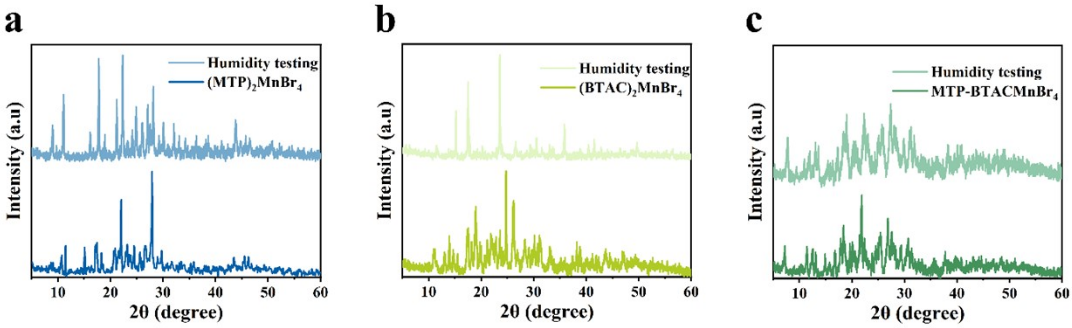

Figure S14. Comparison of XRD characterisation before and after humidity stabilisation for $(MTP)_2MnBr_4$, $(BTAC)_2MnBr_4$, and MTP-BTAC $MnBr_4$ from left to right.

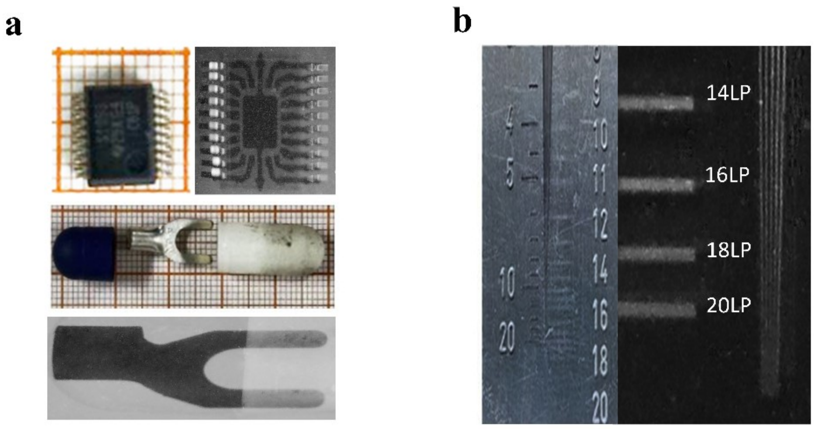

Figure S15. Two-dimensional imaging (a) electronic components (b) Line pair card.

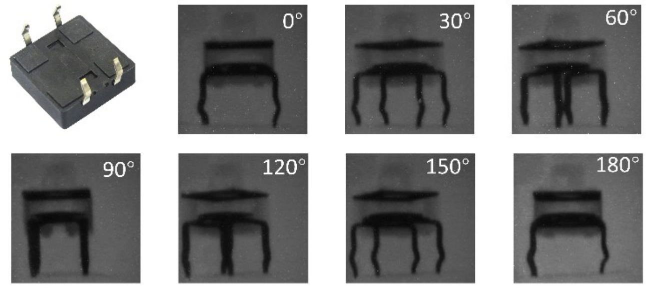

Figure S16. Schematic diagrams of the probe at different angles.

Table S1. Crystal data and structure refinement for the complex.

Compound	MTP-BTACMnBr$_4$
Empirical formula	C29H30.64Br4MnNP
Formula weight	798.73
Crystal system	triclinic
Space group	*P-1*
a/Å	9.5458(5)
b/Å	12.0787(4)
c/Å	14.7429(5)
α/°	103.497(3)
β/°	94.609(4)
γ/°	94.559(4)
V/Å^3	1639.09(12)
Z	2
ρ/g·cm^{-3}	1.618
Crystal size/mm^3	0.44 × 0.23 × 0.16
μ(Gu-Kα)/mm^{-1}	9.576
Data/restraints/parameters	6623/32/392
Goodness-of-fit on F^2	1.008
Reflections collected	20465
Independent reflections	6623
Final R indices [I> 2σ(I)]	R_1 = 0.0861
	wR_2 = 0.2502
R indices (all data)	R_1 = 0.1221
	wR_2 = 0.2988

Table S2. Rheological parameters for $(MTP)_2MnBr_4$, $(BTAC)_2MnBr_4$, MTP-BTAC$MnBr_4$.

Compound	Tm	η (Tm)	Ea
MTP-BTAC$MnBr_4$	136℃	4.0 Pa·s	44.55 KJ·mol^{-1}
$(MTP)_2MnBr_4$	167℃	4.6 Pa·s	21.07 KJ·mol^{-1}
$(BTAC)_2MnBr_4$	151℃	3.1 Pa·s	20.97 KJ·mol^{-1}

Table S3 Comparison of Optical Properties of Different Materials

Scintillators	Light yield/MeV	Detection Limits	Preparation Method
$(ETP)_2MnBr_4$[1]	35000	$103nGy\cdot s^{-1}$	Solution method
$(HTPP)_2MnBr_4$[1]	8600	$185nGy\cdot s^{-1}$	Solution method
$(BTP)_2MnBr_4$[2]	/	$36.2nGy\cdot s^{-1}$	Solution method
$(ETP)_2SbCl_5$ [3]	8500	/	Solution method
BGO	8000	$219nGy\cdot s^{-1}$	Tilting Method
$(C_{38}H_{34}P_2)MnBr_4$[4]	64000	$89.4nGy\cdot s^{-1}$	Solution method
$CsPbBr_3$	10100	$130nGy\cdot s^{-1}$	Solution method
$(MTP)_2MnBr_4$[2]	19771	$213nGy\cdot s^{-1}$	Solution method
$(BTAC)_2MnBr_4$[5]	1741	$1140nGy\cdot s^{-1}$	Solution method
$MTP\text{-}BTACMnBr_4$	23470	$124nGy\cdot s^{-1}$	Solution method

Reference

[1] B. Li, Y. Xu, X. Zhang, K. Han, J. Jin, Z. Xia, Adv. Opt. Mater. 2022, 10,2102793.

[2] B. Li, J. Jin, M. Yin, K. Han, Y. Zhang, X. Zhang, A. Zhang, Z. Xia, Y. Xu, Chem. Sci. 2023, 14, 12238.

[3] M. Yin, B. Li, Z. Yi, Y. Zhang, Z. Xia, Y. Xu, Chem. Commun. 2023, 59,11361.

[4] L. J. Xu, X. S. Lin, Q. Q. He, M. Worku and B. W. Ma, Nat. Commun., 2020, 11.

[5]. X. W. Cai, Y. Y. Zhao, H. Li, C. P. Huang and Z. Zhou, J. Mol. Struct., 2018, 1161, 262-266.